An Electronically-Stabilized Non-Planar Phenalenyl Radical and Its Planar Isomer

Ommid Anamimoghadam, Mark D. Symes, De-Liang Long, Stephen Sproules, Leroy Cronin, Götz Bucher*

WestChem, School of Chemistry, University of Glasgow, Glasgow G12 8QQ, United Kingdom.

ABSTRACT: Stable phenalenyl radicals have great potential as the basis for new materials for applications in the field of molecular electronics. In particular, electronically stabilized phenalenyl species that do not require steric shielding are molecules of fundamental interest, but are notoriously difficult to synthesize. Herein, the synthesis and characterization of two phenalenyl type cations is reported: planar benzo[*i*]naphtho[2,1,8-*mna*]xanthenium (8^+) and helical benzo[*a*]naphtha-[8,1,2-*jkl*]xanthenium (9^+) which can be reduced to the corresponding radicals. Radical 9 represents the first stable, helical phenalenyl radical which does not rely on bulky substituents to ensure its stability. Both cations are water-soluble and the radicals are stable for weeks at room temperature under air. These compounds were characterized crystallographically, and also by NMR, EPR, electrochemistry and electronic spectra. The synthesis of the previously reported compound benzo[5,6]naphthaceno[1,12,11,10-*jklmna*]xanthylium (5^+), the largest oxygen-containing polycyclic hydrocarbon, was undertaken for comparison with 8^+ and 9^+, allowing us to report its crystal structure here for the first time. The different properties of these compounds and their radicals are explained by considering their differing aromaticities using in-depth computational methods.

INTRODUCTION

The quest to identify stable π-conjugated cations and radicals that do not require steric shielding has fascinated chemists for decades.[1-13] These compounds are of great fundamental interest and yet they also have a range of potential applications in photochemistry,[14,15] synthesis,[16,17] materials science,[18-21] spintronics[22-24] and biology.[25,26] In particular, open-shell polycyclic aromatic hydrocarbons have been shown to be promising molecular conductors and spin carriers in the emerging field of organic spin chemistry.[27]

On account of the reactivity of open-shell species, however, it is often necessary to strike a compromise between stability and functionality. For example, in spintronics applications there must be excellent communication between spins, which means that relatively exposed radical centers are desirable;[2] however, this also favors radical dimerization and hence spin inactivation. Incorporation of bulky substituents to prevent dimerization can stabilize such radicals but also isolates the spins, reducing any desirable interactions.

An alternative strategy involves electronic stabilization through incorporation of heteroatoms into the polycyclic aromatic hydrocarbon in order to decrease the spin densities, eliminating the need for bulky groups.[28,29] However, this strategy may not always be favourable for the design of stable π-radicals, for the nature of the polycyclic framework and the position of the incorporated heteroatom(s) are critical for the spin distribution in the molecule. Hence, it is important to consider substructures that are conducive to efficient electronic stabilization such as the phenalenyl moiety, which affords good delocalization and spin-active π-dimerization.[30] Trioxatriangelenum **1**$^+$ (see Figure 1) is a case in point: it is as a remarkably stable pyrylium-based carbenium ion, but due to its polycyclic framework (which incorporates three oxygen atoms), the spin density when **1**$^+$ is reduced by one electron is weakly delocalized, *i.e.* the unpaired electron is not prone to distribute across the phenyl rings. As a result, the one-electron reduction of **1**$^+$ does not result in stable open-shell species but in short-lived radicals that undergo rapid sigma-dimerization between the central carbon atoms.[31,32] The first helical structural analog of **1**$^+$ that can form a stable radical has recently been reported (compound **2**), wherein the radical is protected by sterically-hindering groups.[33,34]

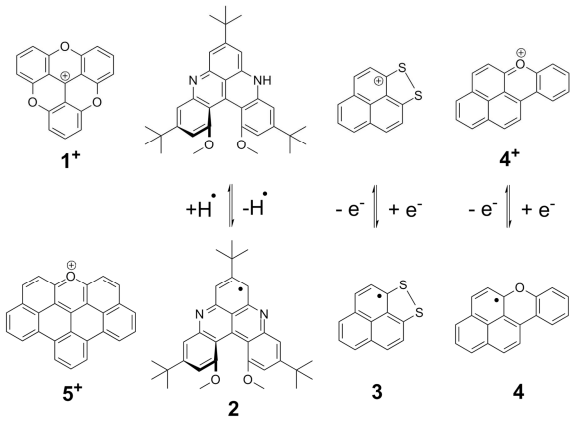

Figure 1 Molecular structures of **1**$^+$, **2**, **3**, **4**$^+$, **4** and **5**$^+$.

Pioneering work in this field has been performed by Haddon *et al.* leading to the synthesis of 1,9-dithiophenalenyl **3** stabilized *via* a disulfide bridge.[28,29] Meanwhile, our groups previously reported the first example of electronic stabilization by an oxygen atom in the phenalenyl species naphtho[2,1,8-*mna*]xanthenyl (**4**), which was generated by reduction of the parent cation.[35] Further planar stable open-shell species have

been prepared by Kubo et al. which are stabilised through delocalization in a large polyaromatic framework. Also bulky substituents were introduced in order to obtain crystals for X-ray structure analysis.[36]

Herein, we describe the synthesis and characterization of two unprecedented phenalenyl species with intriguing properties (benzo[*i*]naphtho[2,1,8-*mna*]xanthenium (**8**$^+$) and benzo[*a*]naphtha-[8,1,2-*jkl*]xanthenium (**9**$^+$), which we compare with **5**$^+$, the largest oxygen-incorporating polycyclic hydrocarbon.[37,] Interestingly, whilst cation **8**$^+$ is planar, cation **9**$^+$ is helical. The radicals of both **8** and **9** could be produced on a preparative scale *via* bulk electrolysis of the corresponding solutions of the cations, and their properties were investigated by EPR spectroscopy and computational methods. Remarkably, the radicals can be stored under an air atmosphere for weeks and both **8** and **9** show astonishingly stable redox behavior under air. To our knowledge, radical **9** represents the first electronically-stabilized non-planar phenalenyl-type radical without sterically hindering groups yet reported. Using EPR spectroscopy analysis supported by simulated spectra, we can confirm distinctly lower spin densities at the α-positions of the phenalenyl skeletons of **8** and **9** compared with 1,9-dithiophenalenyl **3**.[28,29] This decrease of the spin densities suggests a lower tendency for sigma-dimerization of **8** and **9** compared to **3**.

In spite of their large size, both **8**$^+$ and **9**$^+$ are soluble in aqueous media (with the correct choice of counterion), which may serve to make them suitable as dyes or prospective DNA intercalators.[25] Crystal structures were obtained for both **8**$^+$ and **9**$^+$, and these cations exhibit interesting photochemical and redox behavior. We also prepared the previously reported cation of benzo[5,6]naphthaceno-[1,12,11,10-*jklmna*]xanthylium (**5**$^+$) – the largest polycyclic hydrocarbon containing a pyrylium moiety yet synthesized – in order to compare the differences in its structural and electronic properties with those of **8**$^+$ and **9**$^+$. Our investigations of **5**$^+$ have allowed us to obtain the crystal structure of this cation for the first time.

EXPERIMENTAL SECTION

General procedure for the synthesis of 9-(methoxynaphthalenyl)-1*H*-phenalen-1-ones. In a two-neck round bottom flask, Mg in 5 mL of THF was activated with 0.1 mL 1,2-dibromoethane under argon. Then the brominated aryl compound was added to the reaction mixture dropwise in THF by means of a syringe. With slow stirring and heating, the Grignard reagent began to form. After 45 min, 1.00 g (5.5 mmol, 1 eq) of 1*H*-phenalen-1-one dissolved in 10 mL of dry THF was gradually added to the grey solution. The mixture was then refluxed for 4 h. After cooling down to room temperature, the reaction was quenched with 5 mL sat. NH_4Cl solution. Then 20 mL H_2O was added and the product was extracted with EtOAc (3 x 30 mL) and washed with 20 mL brine and dried over $MgSO_4$. When the solvent was evaporated to dryness, the crude product and 1.30 g DDQ (5.6 mmol; 1 eq) were mixed in CH_2Cl_2 and refluxed overnight at 55-60 °C. The next day, the solvent was evaporated by rotary evaporator inside a fumehood. By flash column chromatography using silica and CH_2Cl_2 as the eluent, the desired product was obtained.

Synthesis of 9-(3-methoxynaphthalenyl)-1*H*-phenalen-1-one (6). Following the general procedure, the Grignard reagent was generated from 0.23 g (9.4 mmol; 1.7 eq) Mg and 1.97 g (8.32 mmol; 1.5 eq) 2-bromo-3-methoxynaphthalene dissolved in 5 mL THF at 40-50 °C. After reflux with 1*H*-phenalen-1-one (1 eq) and subsequent oxidation with DDQ, 9-(3-methoxynaphthalenyl)- 1*H*-phenalen-1-one was obtained as a yellow powder in a yield of 36% (0.68 g; 2 mmol). ^{1}H-NMR (400 MHz; $CDCl_3$) δ 3.79 (s, OMe), 6.58 (d, *J* = 9.7 Hz, 1H), 7.22 (s, 1H), 7.33 (ddd, *J* = 8.1, 6.9, 1.2 Hz, 1H), 7.44 (ddd, *J* = 8.2, 6.9, 1.3 Hz, 1H), 7.64 – 7.60 (m, 2H), 7.66 (d, *J* = 8.2 Hz, 1H), 7.69 (d, *J* = 9.8 Hz, 1H), 7.77 (t, *J* = 7.6 Hz, 1H), 7.80 (dd, *J* = 8.2, 0.5 Hz, 1H), 8.06 (dd, *J* = 8.2, 1.0 Hz, 1H), 8.22 (d, *J* = 8.3 Hz, 1H).^{13}C-NMR (100 MHz; $CDCl_3$) δ 55.78 (OMe), 105.49 (Cq), 123.73 (CH), 126.28 (CH), 126.24 (CH), 126.84 (CH), 127.47 (CH), 127.87 (2CH), 128.36 (Cq), 128.86 (Cq), 129.54 (Cq), 130.35 (CH), 131.20 (2CH), 131.73 (CH), 131.84 (CH), 132.28 (Cq), 133.94 (CH), 134.64 (Cq), 134.85 (Cq), 140.35 (Cq), 155.79 (Cq), 185.49 (C=O). UV (in MeCN) – λmax [nm] (log ε): 305 (3.73), 320 (3.75), 360 (3.97). IR (ATIR) ν_{max} [cm^{-1}] 3010-2827 ($CH_{aromatic}$, weak), 1636 (C=O, sharp & intense), 1622, 1598, 1579, 1555, 1503, 1497, 1476, 1458, 1427, 1390, 1385, 1352, 1327, 1248, 1244, 1241 (C-O, sharp), 1198, 1171, 1123, 1107, 1076, 1040. MS (EI+) m/z (rel. intensity): 336 (M^+, 23), 320 (7), 306 (80), 305 (100), 292 (14), 276 (27), 263 (30), 237 (7), 160 (18), 153 (23), 146 (15), 132 (11), 86 (12), 84 (18), 49 (12), 44 (8). HRMS calcd for $C_{24}H_{16}O$: 336.1150, found: 336.1146. Melting point: 194-196 °C (recrystallization from CH_2Cl_2).

Synthesis of 9-(2-methoxynaphthalenyl)-1*H*-phenalen-1-one (7). Following the general procedure, the Grignard reagent was generated from 0.23 g (9.4 mmol; 1.7 eq) Mg and 1.97 g (8.32 mmol; 1.5 eq) 1-bromo-2-methoxynaphthalene dissolved in 5 mL THF at 40-50 °C. After reflux with 1*H*-phenalen-1-one (1 eq) and subsequent oxidation with DDQ 9-(2-methoxynaphthalenyl)-1*H*-phenalen-1-one was obtained as an orange powder in a yield of 70% (1.30 g; 3.86 mmol). ^{1}H-NMR (400 MHz; $CDCl_3$) δ 3.79 (s, OMe), 6.50 (d, *J* = 9.7 Hz, 1H), 7.10 (d, *J* = 8.5 Hz, 1H), 7.20 (ddd, *J* = 8.1, 6.7, 1.3 Hz, 1H), 7.30 (ddd, *J* = 8.1, 6.7, 1.2 Hz, 1H), 7.42 (d, *J* = 9.0 Hz, 1H), 7.59 (d, *J* = 8.3 Hz, 1H), 7.66 (dd, *J* = 8.2, 7.1 Hz, 1H), 7.70 (d, *J* = 9.7 Hz, 1H), 7.80 (d, *J* = 6.3 Hz, 1H), 7.85 (d, *J* = 8.1 Hz, 1H), 7.94 (d, *J* = 9.0 Hz, 1H), 8.10 (d, *J* = 8.2 Hz, 1H), 8.27 (d, *J* = 8.3 Hz, 1H). ^{13}C-NMR (100 MHz; $CDCl_3$) δ 56.85 (OMe), 77.36 (Cq), 113.95 (CH), 123.58 (CH), 124.16 (CH), 126.23 (Cq), 126.35 (CH), 126.54 (CH), 127.97 (Cq), 128.29 (CH), 128.66 (Cq), 128.70 (Cq), 128.94 (CH), 129.44 (Cq), 130.33 (CH), 131.15 (CH), 131.84 (CH), 132.20 (Cq), 132.56 (CH), 134.21 (CH), 140.41 (CH), 142.38 (Cq), 153.06 (Cq), 185.39 (C=O). UV (in MeCN) – λmax [nm] (log ε): 312 (3.75), 341 (3.91), 358 (4.03). IR (ATIR) ν_{max} [cm^{-1}] 3032-2830 ($CH_{aromatic}$, weak), 1630 (C=O, sharp & intense), 1609, 1591, 1545, 1510, 1447, 1380, 1384, 1329, 1253 (C-O, sharp & intense), 1236, 1183, 1176, 1145, 1120, 1084, 1065, 1064. MS (EI+) m/z (rel. intensity): 336 (M^+, 9), 305 (93), 263 (7), 153 (8), 86 (65), 84 (100), 51 (22), 49 (68), 47 (18). HRMS calcd for $C_{24}H_{16}O$: 336.1150, found: 336.1145. Melting point: 203-205 °C (recrystallization from CH_2Cl_2).

General procedure for the synthesis of benzonaphthoxanthenium cations. 0.100 g 9-(2-Methoxyaryl)-1*H*-phenalen-1-one (0.35 mmol) was dissolved in 40 mL CH_2Cl_2 in a round

bottom flask placed in an NaCl/ice bath. Argon was purged through for 5 minutes and the flask was sealed with a septum and supplied with an argon-filled balloon. While stirring, 1.2 mL BBr_3 in heptane (1 M) was slowly added by syringe. The color of the solution changed from orange to dark brown. After 10 minutes, the NaCl/ice-bath was removed and the solution was stirred for 4 hours. After this time, adding 30 mL of H_2O quenched the reaction and dissolved the precipitate giving an orange solution. The aqueous layer was separated and the organic salt in the organic layer was extracted with distilled H_2O (2 x 10 mL). After the aqueous layers were combined and filtered, 5 mL HBF_4 solution was added, yielding a precipitate which was separated by vacuum filtration.

Synthesis of benzo[*i*]naphtho[2,1,8-*mna*]xanthenium tetrafluoroborate (8$^+$). Following the general procedure, 8$^+$ was obtained as a brown powder in a yield of 64%. ^{1}H-NMR (400 MHz; CD_3CN) δ 7.71 (t, *J* = 7.5 Hz, 1H), 7.79 (t, *J* = 7.1 Hz, 1H), 8.15 (d, *J* = 8.4 Hz, 1H), 8.25 (d, *J* = 8.5 Hz, 1H), 8.39 (d, *J* = 9.1 Hz, 1H), 8.43 (t, *J* = 7.7 Hz, 1H), 8.61 (s, 1H), 9.05 (m, 2H), 9.20 (d, *J* = 8.7 Hz, 1H), 9.29 (d, *J* = 9.1 Hz, 1H), 9.36 (d, *J* = 8.7 Hz, 1H), 9.49 (s, 1H). ^{13}C-NMR (100 MHz; CD_3CN) δ 115.63 (Cq), 116.82 (CH), 118.66 (Cq), 120.92 (CH), 122.33 (Cq), 123.45 (CH), 128.40 (CH), 128.48 (CH), 128.63 (Cq), 128.96 (CH), 130.21 (CH), 131.20 (Cq), 131.45 (CH), 131.86 (CH), 132.33 (Cq), 137.30 (Cq), 141.83 (CH), 142.75 (CH), 145.96 (Cq), 148.40 (CH), 149.11 (Cq), 150.36 (CH), 166.07 (C=O$^+$). UV (in MeCN) – λmax [nm] (log ε): 322 (4.15), 363 (3.82), 469 (4.68). IR (ATIR) ν_{max} [cm^{-1}] 3074 ($CH_{aromatic}$, weak), 1603, 1597, 1591, 1566 (C=O+, sharp & intense), 1507, 1472, 1445, 1421, 1360, 1334, 1288, 1239, 1211, 1199, 1163, 1144, 1136, 1027 (B-F, sharp & intense). MS(EI+) m/z (rel. intensity): 305 (100), 276 (21), 274 (9), 231 (5), 219 (5), 187 (8), 181 (7), 169 (8), 153 (13), 131 (10), 119 (8), 85 (6), 69 (16), 44 (83), 40 (15), 36 (22). HRMS calcd for $C_{23}H_{13}O^+$: 305.0966, found: 336.0967. Melting point: 276-280 °C (recrystallization from acetone).

Synthesis of benzo[*a*]naphtho[8,1,2-*jkl*]xanthenium tetrafluoroborate (9$^+$). Following the general procedure, 9$^+$ was obtained as a brown powder in a yield of 67%.^{1}H-NMR (400 MHz; CD^3CN) δ 7.95 (ddd, *J* = 8.0, 7.1, 1.0 Hz, 1H), 8.07 (ddd, *J* = 8.5, 7.1, 1.4 Hz, 1H), 8.26 (d, *J* = 9.1 Hz, 1H), 8.33 (dd, *J* = 8.0, 1.2 Hz, 1H), 8.58 (t, *J* = 7.7 Hz, 1H), 8.60 (d, *J* = 9.1 Hz, 1H), 8.69 (d, *J* = 9.1 Hz, 1H), 9.18 – 9.10 (m, 2H), 9.28 (d, *J* = 8.5 Hz, 1H), 9.34 (d, *J* = 9.1 Hz, 1H), 9.39 (d, *J* = 9.1 Hz, 1H), 9.61 (d, *J* = 9.1 Hz, 1H). ^{13}C-NMR (100 MHz; CD_3CN) δ 117.00 (Cq), 117.64 (Cq), 118.65 (CH), 120.11 (CH), 121.84 (Cq), 126.27 (CH), 128.26 (CH), 129.20 (Cq), 129.24 (Cq), 129.97 (CH), 130.57 (Cq), 131.39 (CH), 131.43 (CH), 131.45 (CH), 133.17 (Cq), 139.27 (CH), 140.42 (CH), 140.95 (CH), 144.32 (Cq), 146.73 (CH), 146.88 (CH), 155.76 (Cq), 161.38 (C=O$^+$). UV (in MeCN) – λmax [nm] (log ε): 311 (4.91), 505 (5.12). IR (ATIR) ν_{max} [cm^{-1}] 3061, 1617, 1602, 1577, 1564, 1545, 1518, 1495, 1472, 1431, 1412, 1382, 1350, 1324, 1279, 1246, 1236, 1224, 1192, 1176, 1147, 1137, 1115, 1091, 1032, 983. MS(EI+) m/z (rel. intensity): 305 (100), 276 (28), 274 (10), 153 (9), 152 (8), 137 (7), 69 (3), 44 (4), 40 (3). HRMS calcd for $C_{23}H_{13}O^+$: 305.0966, found: 305.0972. Melting point: 273-275 °C (recrystallization from acetone).

Synthesis of benzo[5,6]naphthaceno[1,12,11,10-*jklmna*]xanthylium tetrafluoroborate (5$^+$). In a two-neck round bottom flask, 300 mg (0.8 mmol; 1 eq) of 14-phenyl-14*H*-dibenzo[*a,j*]xanthene was dissolved in 25 mL of glacial acetic acid under reflux at 100 °C. Then 0.05 mL (1 mmol; 1.2 eq) of Br_2 mixed with 5 mL acetic acid were added dropwise to the solution and the reaction was refluxed for 30 minutes. After cooling down the red solution, the precipitate was separated by vacuum filtration. The crude product was recrystallized from acetic acid resulting in 14-phenyldibenzo[a,j]xanthenium bromide as red-orange crystals with a golden lustre in a yield of 59% (216 mg; 0.5 mmol; lit.: 83%[37]). Without further purification, the batch of 14-phenyldibenzo[*a,j*]xanthenium bromide was dissolved in 60 mL of MeCN and 5 mL of HBF_4 solution (48 wt. % in H_2O). After UV irradiation overnight, black needles of 5$^+$ were obtained in a yield of 30% over two steps (112 mg; 0.3 mmol). This compound analyzed as per the analogous bromide salt previously reported.[37] IR (ATIR) ν_{max} [cm^{-1}] 3055 ($CH_{aromatics}$, weak), 1617, 1605, 1582 (C=O$^+$, intense), 1464, 1431, 1395, 1353, 1335, 1314, 1264, 1251, 1241, 1210, 1199, 1144, 1077, 1022 (B-F, intense). MS (FAB+) m/z (rel. intensity): 353 (36), 121 (30), 91 (10), 77 (10), 44 (100). Melting Point: > 360 °C (recrystallization from acetonitrile). HRMS calcd for $C_{27}H_{13}O$: 353.0966, found: 353.0968.

Computational methods: All calculations were performed using the *Gaussian09* suite of programmes.[38] Optimizations were performed using the B3LYP[39] and M05-2X[40] density functional methods, in combination with 6-31G** and 6-31+G* basis sets.[41] All minima were characterized as such by performing a vibrational analysis.

RESULTS AND DISCUSSION

Our synthetic methodology is shown in Scheme **1**, and is based on a 4-step synthesis *via* the two new precursors 9-(3-methoxynaphthalenyl)-1*H*-phenalen-1-one **6** (which gives 8$^+$) and 9-(2-methoxynaphthalenyl)-1*H*-phenalen-1-one **7** (which leads to 9$^+$).

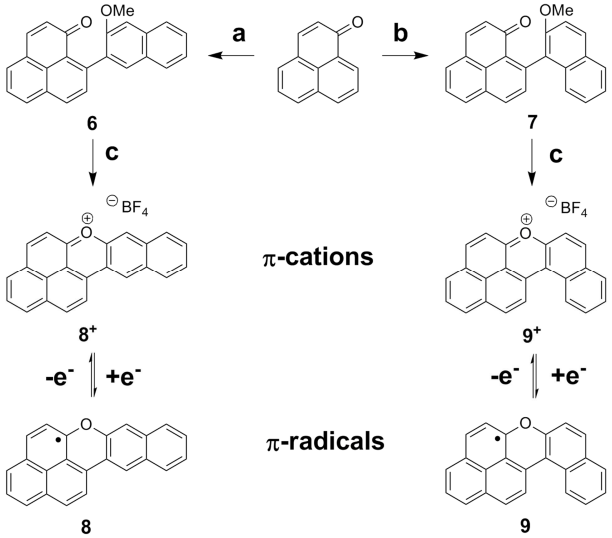

Scheme 1 Synthesis of phenalenyl cations and radicals; a) i. ((3-methoxynaphthalen-2-yl)magnesium bromide, THF, rt; ii.) DDQ, CH_2Cl_2, reflux. b) i. (2-methoxynaphthalen-1-yl)magnesium bromide, THF, rt; ii. DDQ, CH_2Cl_2, reflux. c) i. BBr_3, CH_2Cl_2, 0°-rt; ii. HBF_4 (48 wt. % in H_2O).

Both precursors were synthesized by a Michael-type Grignard addition to the 9-C position of 1*H*-phenalenone, with subsequent oxidation using DDQ.[42] This procedure gave **6** and **7** in yields of 36% and 70% respectively over two steps. Subsequently, demethylation using BBr_3 in CH_2Cl_2 resulted in the corresponding 9-(hydroxynaphthalenyl)-1*H*-phenalen-1-ones which underwent rapid cyclization in presence of water to give $\mathbf{8}^+$ and $\mathbf{9}^+$ with bromide as the counterion. These salts were soluble in water and were isolated in pure form by extraction into aqueous solution followed by precipitation as the tetrafluoroborate salts, yielding $\mathbf{8}^+$ (64%) and $\mathbf{9}^+$ (67%).

Cation $\mathbf{8}^+$ crystallized from acetone in a triclinic system with space group P-1 (see, Table S4 and Figure S6 in the Supporting Information). The molecules in this structure are arranged in π-π stacking arrays separated by distances of between 3.286-3.389 Å. $\mathbf{8}^+$ can be considered planar with a negligibly small torsion angle of 1.068° in the bay region. Cation $\mathbf{9}^+$ also crystallized from acetone in a triclinic system with space group P-1 (see Table S5 and Figure S7 in Supporting Information) as a racemic mixture of the possible enantiomers, P and M. Due to its *fjord* region, $\mathbf{9}^+$ exhibits a helical geometry with a torsion angle of 28.579°.

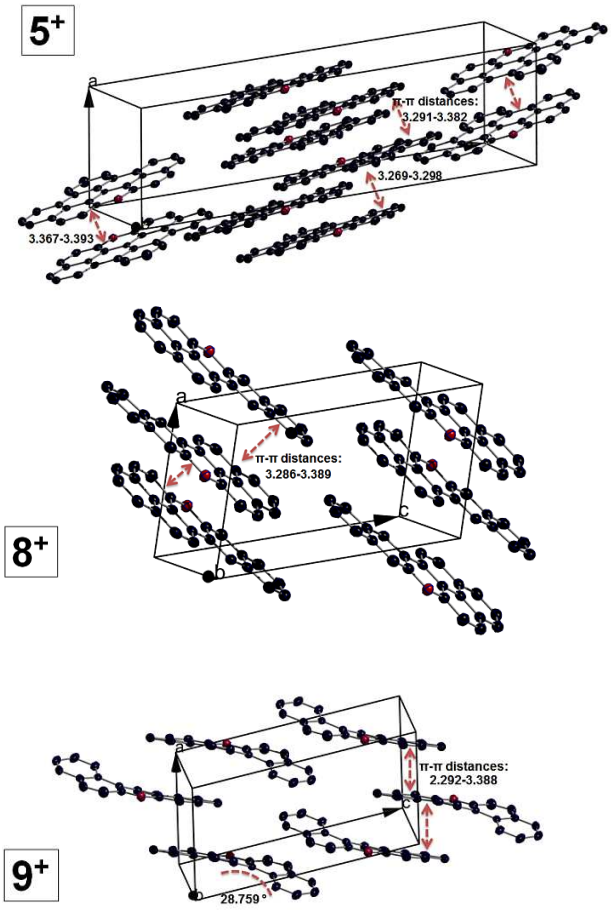

Figure 2 Illustration of π-π stacking arrangements of compounds $\mathbf{5}^+$, $\mathbf{8}^+$ and $\mathbf{9}^+$ obtained from X-ray structure analysis. Counterions are not displayed for clarity.

Meanwhile, the synthesis of $\mathbf{5}^+$ was achieved using a slightly modified literature procedure (see Experimental Section for details),[37] resulting in crystals of $\mathbf{5}^+$ as the tetrafluoroborate salt that proved suitable for X-ray diffraction. Analysis of the resulting X-ray structure of $\mathbf{5}^+$ (see Table S6 and Figure S5 in Supporting Information) shows an arrangement in a triclinic system, with antiplanar π-stacking interactions giving rise to two parallel columns in the unit cell. Between these columns antiplanar π-π interacting pairs of $\mathbf{5}^+$ are arranged with a separation of 3.367-3.393 Å. The molecule can be considered planar with negligibly small torsion angles of 1.067° and 0.525° in the bay regions. Illustrations of the assembly of $\mathbf{5}^+$, $\mathbf{8}^+$ and $\mathbf{9}^+$ obtained from X-ray structure analysis are displayed below in Figure 2.

In terms of electronic properties, cation $\mathbf{8}^+$ shows a red shift of 13 nm in its absorption spectrum compared with the previously reported cation $\mathbf{4}^+$ on account of the more extended polyaromatic framework in $\mathbf{8}^+$ (Figure 3). The same trend is also evident with $\mathbf{9}^+$, but to an even greater extent. $\mathbf{9}^+$ shows a broader absorption than $\mathbf{8}^+$ with a maximum at 505 nm (a bathochromic shift of 36 nm compared with $\mathbf{8}^+$). This result is unexpected and intriguing, given that the benzene-fused skeleton is less linear in $\mathbf{9}^+$ than it is in $\mathbf{8}^+$. According to Clar's approach, $\mathbf{9}^+$ comprises more Robinson rings than $\mathbf{8}^+$ and hence $\mathbf{9}^+$ should exhibit a higher aromaticity when compared to $\mathbf{8}^+$. This in turn would imply that $\mathbf{9}^+$ should absorb shorter wavelengths of light than $\mathbf{8}^+$. However, as this is clearly not the case, we propose that the geometry and the position of the pyrylium ring in $\mathbf{9}^+$ are disrupting this aromaticity and causing a bathochromic shift to manifest instead.

The different intensities of fluorescence emission from $\mathbf{4}^+$, $\mathbf{8}^+$ and $\mathbf{9}^+$ could be observed with the naked eye (Figure 3, inset). The fluorescence emission spectra (Figure 3) show the emission of $\mathbf{4}^+$ (2.8×10^{-5} mol/L), $\mathbf{8}^+$ (1×10^{-5} mol/L) and $\mathbf{9}^+$ (3.1×10^{-6} mol/L) upon excitation at 435 nm, 465 nm and 505 nm, respectively. $\mathbf{4}^+$ emits between 450 and 600 nm with a maximum at 471 nm giving a Stokes shift of 15 nm. $\mathbf{8}^+$ also emits up to 600 nm, however, with a considerably lower intensity. The maximum peak lies at 516 nm, which corresponds to a Stokes shift of 47 nm. A broad emission between 510 nm and 690 nm can be observed for $\mathbf{9}^+$ with a maximum peak at 562 nm, indicating a red shift (and a higher intensity) compared with $\mathbf{8}^+$. Cation $\mathbf{8}^+$ displayed a relatively low intensity compared to $\mathbf{4}^+$ and $\mathbf{9}^+$. This can be attributed to collisional quenching by π-π stacking interactions. In the case of $\mathbf{9}^+$, the helical structure results in the minimization of π-π interactions and hence a greater emission intensity.

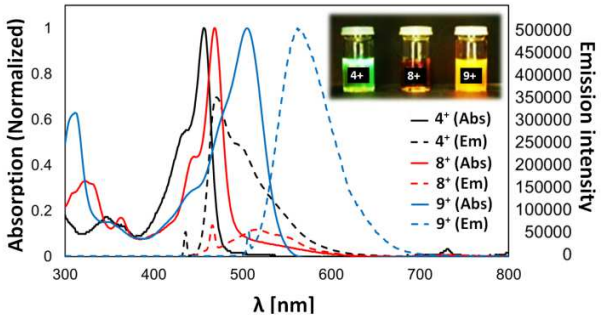

Figure 3 UV-visible and fluorescence spectra of $\mathbf{4}^+$, $\mathbf{8}^+$ and $\mathbf{9}^+$ in MeCN.

The cyclic voltammogram (CV) of $\mathbf{8}^+$ is shown as the black dashed line in Figure 4 (see Supporting Information for electrochemical methods). Two reversible redox waves are evident centered around –0.43 V and –1.53 V *vs.* ferrocene/ferrocenium. The least negative of these waves corre-

sponds to the formation of the neutral radical species, and the second to the formation of the 8^- mono-anion. A CV of 9^+ under the same conditions is shown for comparison as the solid red line in Figure 4. Again, two well-defined reversible waves are evident in the absence of oxygen, occurring at roughly –0.59 V and –1.67 V *vs.* ferrocene/ferrocenium. Compared to $4^{+(35)}$, these redox process for 8^+ are both somewhat less negative. In the case of 4^+, $E_{cation/radical}$ = –0.52 V for the formation of the neutral radical from the cation, whilst the reduction of this radical to give the anion occurred at $E_{radical/anion}$ = –1.66 V. This indicates that 8^+ is easier to reduce than 4^+, both in the cationic and neutral radical forms, possibly on account of the greater degree of delocalization in 8^+. For 9^+, formation of the neutral radical species is harder than in the case of 4^+, but formation of the cation occurs at roughly the same potential. In contrast, compound 5^+ showed significantly more cathodic shifts for both its corresponding waves with $E_{cation/radical}$ = –0.96 V and $E_{radical/anion}$ = –1.80 V (see Figure S1 in the Supporting Information).

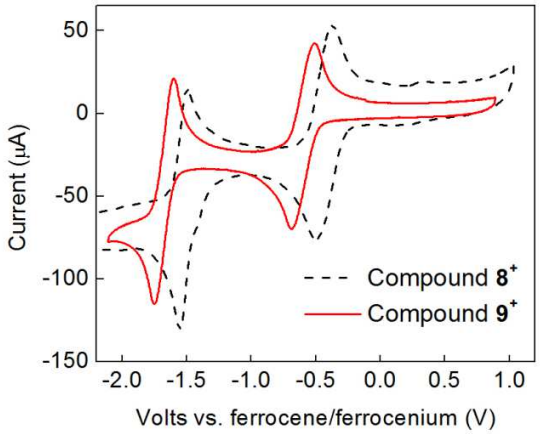

Figure 4 Cyclic voltammograms of 8^+ and 9^+ at room temperature obtained at scan rates of 100 mV s^{-1} on a glassy carbon working electrode of area 0.071 cm^{-2}. Peaks are referenced to the Fc/Fc^+ couple (wave not shown).

When cyclic voltammograms of 8^+ and 9^+ were recorded under an air atmosphere, the first redox waves for both compounds (corresponding to the cation/radical redox processes) showed very good reversibility, which is indicative of a lack of side reactions. After 2000 cycles at a scan rate of 100 mV/s, no depletion of the first redox wave for either 8^+ or 9^+ was observed (Figure 5). These results could be reproduced using the same samples after one week. Hence radicals **8** and **9** may be capable of acting as stable paramagnetic redox partners without the need for an inert atmosphere. Hence these radicals are stable to redox cycling in air, with no significant degradation evident by CV over the course of several hours. Other radicals (*e.g.* DPPH, TEMPO and verdazyl radicals) are also stable over long periods of time. However, in these cases the spin density is concentrated on heteroatoms (O and N) and bulky substituents are required in order to prevent deleterious side reactions occurring. This is in contrast to the carbon-based, delocalized radicals stabilised through electronics that we report herein. The second redox waves for both **8** and **9** (corresponding to the radical/anion redox couples) were found to be irreversible when probed under air.

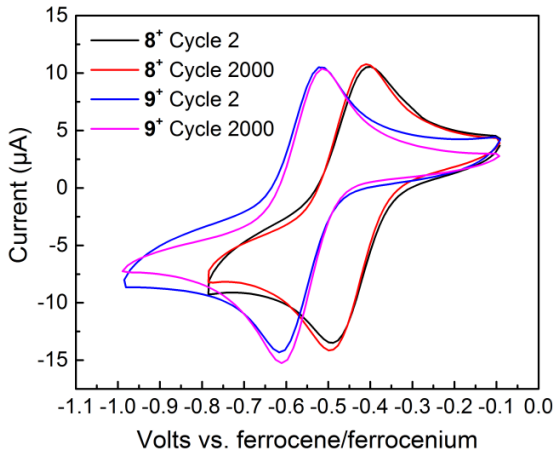

Figure 5 Cyclic voltammograms of compounds 8^+ and 9^+ at room temperature and under an air atmosphere at a scan rate of 100 mV s^{-1} on a glassy carbon electrode of area 0.071 cm^2. Peaks are referenced to the Fc/Fc^+ couple. Both compounds were cycled 2000.

The radicals **8** and **9** were formed electrochemically by bulk electrolysis of solutions of the corresponding cations at –1.0 V *vs.* ferrocene/ferrocenium with 0.1 M $N(Bu)_4BF_4$ as the supporting electrolyte. Upon complete reduction to the radicals, the colour of the solutions had turned to yellow and dark red for **8** and **9**, respectively. The UV/Vis spectra showed the full depletion of the absorption peaks indicative of the cations and suggested the presence of the corresponding radicals (see Figure S2 in the Supporting Information). In the case of **8**, three maxima were detected with values at 403 nm, 441 nm and 465 nm including a shoulder at 494 nm. Further absorption peaks were evident between 300 nm and 380 nm with peaks at 320 nm, 335 nm and 362 nm which appear to be similar to the absorption of the corresponding cation. The UV spectrum of **9** shows strong absorption between 320 nm and 450 nm with a clear maximum peak at 360 nm. Furthermore a broad shoulder with moderate absorption can be found between 455 nm and 565 nm. It is noteworthy that the absorption spectrum of radical **9** is very similar to the absorption spectrum of radical **4** published previously.[35]

Product solutions from completed bulk electrolyses were investigated by EPR spectroscopy, which confirmed that radicals had been formed. Signals with g-values of 2.00258 were obtained for **8** and 2.0028 for **9**, which are close to that of a free electron (g = 2.002319). Figure 6 shows the coupling patterns in which the total number of lines, hypothetically made up of $(2 \times 1 \times ½ + 1)^{13}$ = 8192 lines, cannot be observed due to the limited resolution. Nonetheless, by computational methods Mulliken spin densities (calculated at the M05-2X/6-31G** level of theory – see Tables S2 & S3 in the Supporting Information) could be assigned to the radical centers. These spin densities correlate with the hyperfine coupling constants, allowing spectra which match with the experimental spectra to be simulated (see Figure 6 including Figure S3 & S4 in the Supporting Information). It is noteworthy that the spin densities at the α-position of the phenalenyl skeleton are below the corresponding spin densities of 1,9-dithiophenalenyl **3** (0.51 mT & 0.54 mT)[28,29] indicative of a higher stabilization of **8** and **9** compared with **3**.

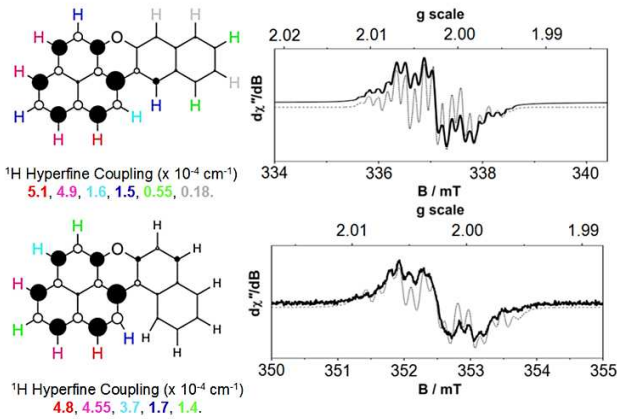

Figure 6 X-band EPR spectra of **8** and **9** in DMSO at 293 K (experimental conditions for **8**: frequency, 9.4481 GHz; power, 0.63 mW; modulation, 0.02 mT; experimental conditions for **9**: frequency, 9.8812 GHz; power, 0.63 mW; modulation, 0.02 mT). Experimental data are shown by the black traces and the simulations as grey lines.

Using the bond lengths obtained from the X-ray data, Harmonic Oscillating Model of Aromaticity (HOMA)[43] indices were calculated using the HOMA model formula.[44] In addition, Nucleus Independent Chemical Shift (NICS)[45] values of dummy atoms centered 1 Å above the plane of benzenoid rings were computed based on the B3LYP level of theory using a basis set of 6-31+G*. For compound $\mathbf{5}^+$, the pyrylium ring exhibits the lowest HOMA and NICS values of 0.42 and –4.21 due to the perturbation caused by the oxygen atom (see Figure 7). The bond lengths of C_x-O and C_y-O are identical (1.362 Å). The degrees of aromaticity for the inner rings B and F are distinctly lower compared to those of the outer rings (see Table S1 in Supporting Information). Rings A, E and G exhibit the highest degrees of aromaticity. The inner rings are less aromatic than rings C and D, hence $\mathbf{5}^+$ appears to comprise two naphthalene substructures at the outer frames (A-C and D-E) characterized by their electronic structure. Thus there appears to be less phenalenyl character in $\mathbf{5}^+$ than in $\mathbf{8}^+$ or $\mathbf{9}^+$, which could explain the more cathodic reduction potentials of $\mathbf{5}^+$ relative to $\mathbf{8}^+$ and $\mathbf{9}^+$ (less phenalenyl character and so less stabilization through delocalization).

The evaluation of the aromaticity for $\mathbf{8}^+$ shows that the three rings A, B and C resemble rather more the electronic structure of phenalenyl than it is the case for $\mathbf{5}^+$. The naphthalene unit annulated with the pyrylium ring has a slightly higher degree of aromaticity in ring D compared to ring E. It is noteworthy that the C_x-O bond is distinctly shorter than the C_y-O bond indicating that a nucleophile (*e.g.* hydroxide) would not be prone to attack the ring at the C_y position. This is consistent with Clar's rule, as otherwise a loss of aromaticity would result, which can be depicted by depletion of one Robinson ring. The tendency for a nucleophilic attack at the C_x and C_b positions is additionally decreased due to the conjugation provided by the phenalenyl unit, resulting in an optimal stabilization of the whole molecule.

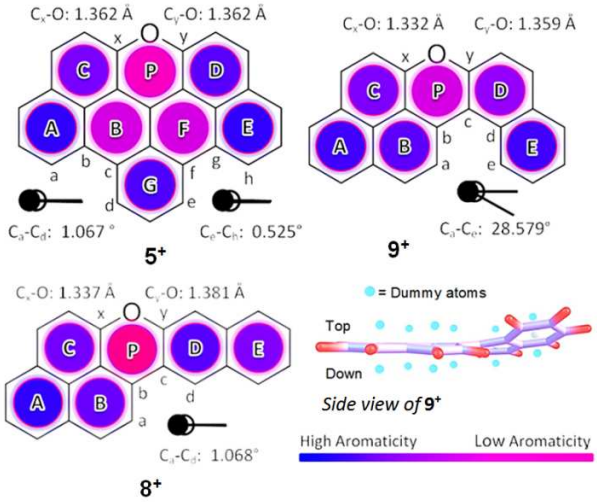

Figure 7 Molecular structures of $\mathbf{5}^+$, $\mathbf{8}^+$ and $\mathbf{9}^+$ showing C-O distances and torsion angles in the bay and fjord regions. HOMA values are calculated using bond lengths from X-ray data analysis. NICS values are obtained from calculation based on the B3LYP level of theory using a basis set 6-31+G*. In the case of $\mathbf{9}^+$, the NICS values for both sides of the molecule were computed using dummy atoms which are 1 Å distant from the center of each ring.

As $\mathbf{9}^+$ is non-planar, a statement about the aromaticity based on the electromagnetic parameters using NICS values is considered for both sides of the plane at a distance of 1 Å from the center of each 6-membered ring. The pyrylium ring exhibits a slight enhancement of aromaticity compared with the ones for $\mathbf{8}^+$ and $\mathbf{5}^+$ which is observed by considering the HOMA index and NICS values of 0.52 and –5.93/–7.22, respectively. Contrary to $\mathbf{8}^+$, the benzene ring E in $\mathbf{9}^+$ is more aromatic than ring D adjacent to the pyrylium ring. Comparing the planarities of the pyrylium rings in all the presented molecules, the root mean square deviations of fitted atoms in these rings are below 0.01 Å, indicating a negligible geometrical effect on the degrees of aromaticity.

We propose that a more pronounced oxonium-carbenium resonance structure is found on the side of the phenalenyl unit in cations $\mathbf{8}^+$ and $\mathbf{9}^+$ (when compared to cation $\mathbf{5}^+$) represented by the bond lengths of 1.337 and 1.332 Å, respectively. Hence, it appears that cations $\mathbf{8}^+$ and $\mathbf{9}^+$ have the propensity to resemble the electronic structure of the chromophore compound phenalenone.[46] In contrast, $\mathbf{5}^+$ shows very low degrees of aromaticity in the inner rings C and F. Thus a delocalization pattern similar to a phenalenyl unit comparable with $\mathbf{8}^+$ and $\mathbf{9}^+$ is non-existent, *i.e.* $\mathbf{5}^+$ can be classified as a non-phenalenyl type cation. This aromaticity evaluation may indicate that compounds $\mathbf{8}^+$ and $\mathbf{9}^+$ do not represent typical electronic structures of xanthenyl species due to the presence of the phenalenyl skeleton. In contrast with xanthenyl, $\mathbf{8}^+$ and $\mathbf{9}^+$ are not prone to undergo nuclueophilic attack on the 4- position of the pyrylium ring. Hence, we demonstrate that a phenalenyl unit combined with pyrylium derivatives can result in complementary electronic systems, where the two α-positions of the phenalenyl moiety represent the commonly reactive sites of the pyrylium ring (the 2´ and the 4´ positions). Such a situation was previously suggested by Haddon and co-workers as a result of their elegant work with 1,9-dithiophenalenyl **3**, which incorporates a 1,2-dithiolyl ring.[28,29] However, we note that the oxidized forms of the phenalenyl radicals presented herein also represent fascinating dyes and

hence may also open up new avenues of research in the area of phenalenyl chemistry.

CONCLUSIONS

In conclusion, we have demonstrated that our synthetic protocol gives access to a new series of π-amphoteric species of interest in the field of phenalenyl chemistry, including the first example of a helical phenalenyl radical stabilized only by the incorporation of a heteroatom ever reported. Our results highlight the remarkable stability of these electronically-stabilized radicals which can be stored under air for weeks without noticeable degradation. It is noteworthy that phenalenyl and pyrylium species on their own give short-lived radicals upon one-electron reduction under air, which subsequently undergo side-reactions such as sigma-dimerization. Hence, the high reversibility of the cation-radical redox processes under air reported herein suggests an intriguing complementary stabilization between the phenalenyl and pyrylium substructures affording novel, stable phenalenyl-type species which may act as dyes or stable open-shell species depending on their redox states. Although $\mathbf{8}^{+}$ and $\mathbf{9}^{+}$ have an electronic structure based on phenalenyl (in contrast to $\mathbf{5}^{+}$), the overall polyaromatic frameworks of these two compounds represent two distinct scaffolds due to their differing shapes. Interestingly the absorption of $\mathbf{9}^{+}$ is distinctly red shifted compared with that of $\mathbf{8}^{+}$ despite its less linear benzene-fused skeleton. The non-planar topology of $\mathbf{9}^{+}$ prevents efficient fluorescence quenching by π-π interactions compared with its isomer $\mathbf{8}^{+}$. This, in combination with its water solubility, makes $\mathbf{9}^{+}$ a promising candidate as a dye for DNA intercalation studies. Future work in our laboratory will endeavour to focus on the potential applications of these compounds and on preparing even more complex and topologically interesting cations and radicals of this sort.

ASSOCIATED CONTENT

Supporting Information

Detailed experimental protocols, additional electrochemical, electronic, EPR, computational and crystallographic data, as well as characterisation of all new compounds reported herein. This material is available free of charge via the Internet at http://pubs.acs.org.

AUTHOR INFORMATION

Corresponding Author

* goebu@chem.gla.ac.uk

Author Contributions

The manuscript was written through contributions of the authors.

ACKNOWLEDGMENTS

MDS thanks the University of Glasgow for a Kelvin Smith Research Fellowship. This work was supported by the University of Glasgow and the EPSRC. LC thanks the Royal Society for a Wolfson Merit Award.

REFERENCES

(1) Reid, D. H. *Q. Rev. Chem. Soc.* **1965**, 19, 274-302.
(2) Sun, Z.; Wu, J. *J. Mater. Chem.* **2012**, 22, 4151-4160.
(3) Bosson, J.; Gouin, J.; Lacour, J. *Chem. Soc. Rev.* **2014**, 43, 2824-2840.
(4) Herse, C.; Bas, D.; Krebs, F. C.; Bürgi, T.; Weber, J.; Wesolowski, T.; Laursen, B. W.; Lacour, J. *Angew. Chem. Int. Ed.* **2003**, 42, 3162-3166.
(5) O´Connor, G. D.; Troy, T. P.; Roberts, D. A.; Chalyavi, N.; Fückel, B.; Crossley, M. J.; Nauta, K.; Stanton, J. F.; Schmidt, T. W. *J. Am. Chem. Soc.* **2011**, 133, 14554-14557.
(6) Mukherjee, A.; Sen, T. K.; Ghorai, P. Kr.; Mandal, S. K. *Scientific Reports* **2013**, 3, 2821.
(7) Small, D.; Zaitsev, V.; Jung, Y.; Rosokha, S. V.; Head-Gordon, M.; Kochi, J. K. *J. Am. Chem. Soc.* **2004**, 126, 13850-13858.
(8) Kuratsu, M.; Kozaki, M.; Okada, K. *Angew. Chem.* **2005**, 44, 4056-4058.
(9) Cyrański, M. K.; Havenith, R. W. A.; Dobrowolski, M. A.; Gray, B. R.; Krygowski, T. M.; Fowler, P. W.; Jenneskens, L. W. *Chem. Eur. J.* **2007**, 13, 2201-2207.
(10) McLachlan, A. D. *Mol. Phys.* **1960** 3, 233-252.
(11) Martin, J. C.; Smith, R. G. *J. Am. Chem. Soc.* **1964**, 86(11), 2252-2256.
(12) Bowie, W. T.; Feldman, M. R. *J. Am. Chem. Soc.* **1977**, 99, 4721-4726.
(13) Faldt, A.; Krebs, F. C.; Thorup, N. *J. Chem. Soc.* **1997**, Perkin Trans 2, 2219-2228.
(14) Sørensen, T. J.; Laursen, B. W. *J. Org. Chem.* **2010**, 75, 6182-6190.
(15) Laursen, B. W.; Sørensen, T. J. *J. Org. Chem.* **2009**, 74, 3183-3185.
(16) Nicolas, C.; Lacour J. *Org. Lett* **2006**, 8(19), 4343-4346.
(17) Sen, T. K.; Mukherjee, A.; Modak, A.; Ghorai, P. Kr.; Kratzert, D.; Granitzka, M.; Stalke, D.; Mandal, S.K. *Chem. Eur. J.* **2012**, 18, 54-58.
(18) Krebs, F. C.; Spanggaard, H.; Rozlosnik, N.; Larsen, N. B.; Jørgensen, M. *Langmuir* **2003**, 19, 7873-7880.
(19) Pariyar, A.; Vijaykumar, G.; Bhunia, M.; Dey, S. Kr.; Singh, S. K.; Kurungot, S.; Mandal, S. K. *J. Am. Chem. Soc.* **2015**, 137, 5955-5960.
(20) Chi, X.; Itkis, M. E.; Reed, R. W.; Oakley, R. T.; Cordes, A. W.; Haddon, R. C. *J. Phys. Chem. B* **2002**, 106, 8278-8287.
(21) Morita, Y.; Miyazaki, E.; Yokoyama, T.; Kubo, T.; Mochizuki, E.; Kai, Y.; Najasuji, K. *Synthetic Metals* **2003**, 135-136, 617-618.
(22) Itkis, M. E.; Chi, X.; Cordes, A. W.; Haddon, R. C. *Science* **2002**, 296, 1443-1445.
(23) Urdampilleta, M.; Klyatskaya, S.; Cleuziou, J.-P.; Ruben, M.; Wernsdorfer, W. *Nat. Mater.* **2011**, 10, 502-506.
(24) Sanvito, S. *Nat. Mater.* **2011**, 10, 484-485.
(25) Reynisson, J.; Schuster, G. B.; Howerton, S. B.; Williams, L. D.; Barnett, R. N.; Cleveland, C. L.; Landman, U.; Harrit, N.; Chaires, J. B. *J. Am. Chem. Soc.* **2003**, 125, 2072-2083.
(26) Pothukuchy, A.; Mazzitelli, C. L.; Rodriguez, M. L.; Tuesuwan, B.; Salazar, M.; Brodbelt, J. S.; Kerwin, S. M. *Biochemistry* **2005**, 44, 2163-2172.
(27) Morita, Y.; Suzuki, S.; Sato, K.; Takui, T. *Nature Chem.* **2011**, 3, 197-204.
(28) Haddon, R. C.; Wudl, F.; Kaplan, M. L.; Marshall, J. H.; Cais, R. E.; Bramwell, F. B. *J. Am. Chem. Soc.* **1978**, 100(24), 7629-7633.
(29) Beer, L.; Mandal, S. K; Reed, R. W.; Oakley, R. T.; Tham, F. S.; Donnadieu, B.; Haddon, R. C. *Cryst. Growth Des.* **2007**, 7(4), 802-809.
(30) Suzuki, S.; Morita, Y.; Fukui, K.; Sato, K.; Shiomi, D.; Takui, T.; Nakasuji, K. *J. Am. Chem. Soc.* **2006**, 128(8), 2530-2531.
(31) Sabacky, M. J.; Johnson Jr., C. S.; Smith, R. G.; Gutowsky, H. S.; Martin, J. C. *J. Am. Chem. Soc.* **1967**, 89(9), 2054-2058.
(32) Bowie, W. T.; Feldman, M. R. *J. Am. Chem. Soc.* **1977**, 99, 4721-4726.
(33) Torricelli, F.; Bosson, J.; Besnard, C.; Chekini, M.; Bürgi, T.; Lacour, J. *Angew. Chem.* **2013**, 52, 1796-1800.
(34) Ueda, A.; Wasa, H.; Suzuki, S.; Okada, K.; Sato, K.; Takui, T.; Morita, Y. *Angew. Chem. Int. Ed.* **2012**, 51, 6691-6695.
(35) Anamimoghadam, O.; Symes, M. D.; Busche, C.; Long, D.-L.; Caldwell, S. T.; Flors, C.; Nonell, S.; Cronin, L.; Bucher, G. *Org. Lett.* **2013**, 15, 2970-2973.
(36) Kubo, T.; Katada, Y; Shimizu, A.; Hirao, Y.; Sato, K.; Takui, T.; Uruichi, M.; Yakushi, K.; Haddon, R.C. *J. Am. Chem. Soc.* **2011**, 133, 14240-14243.
(37) Wu, D.; Pisula, W.; Haberecht, M. C.; Feng, X.; Müllen, K. *Org. Lett.* **2009**, 11, 5686-5689.
(38) Gaussian 09, Revision D.01, Frisch, M. J.; Trucks, G. W.; Schlegel, H. B.; Scuseria, G. E.; Robb, M. A.; Cheeseman, J. R.; Scalmani, G.; Barone, V.; Mennucci, B.; Petersson, G. A.; Nakatsuji, H.; Caricato, M.; Li, X.; Hratchian, H. P.; Izmaylov, A. F.; Bloino, J.; Zheng, G.; Sonnenberg, J. L.; Hada, M.; Ehara, M.; Toyota, K.; Fukuda, R.; Hasegawa, J.; Ishida, M.; Nakajima, T.; Honda, Y.; Kitao, O.; Nakai, H.; Vreven, T.; Montgomery, J. A., Jr.; Peralta, J. E.; Ogliaro, F.; Bearpark, M.; Heyd, J. J.; Brothers, E.; Kudin, K. N.; Staroverov, V. N.; Kobayashi, R.; Normand, J.; Raghavachari, K.; Rendell, A.; Burant, J. C.; Iyengar, S. S.; Tomasi, J.; Cossi, M.; Rega, N.; Millam, J. M.; Klene, M.; Knox, J. E.; Cross, J. B.; Bakken, V.; Adamo, C.; Jaramillo, J.; Gomperts, R.; Stratmann, R. E.; Yazyev, O.; Austin, A. J.; Cammi, R.; Pomelli, C.; Ochterski, J. W.; Martin, R. L.; Morokuma, K.; Zakrzewski, V. G.; Voth, G. A.; Salvador, P.; Dannenberg, J. J.; Dapprich, S.; Daniels, A. D.; Farkas, Ö.; Foresman, J. B.; Ortiz, J. V.; Cioslowski, J.; Fox, D. J. Gaussian, Inc., Wallingford CT, 2009.
(39) Becke, A. D. *J. Chem. Phys.* **1993**, 98, 5648-5652.
(40) Zhao, Y.; Schultz, N. E.; Truhlar, D. G. *J. Chem. Theory and Comput.*, **2006**, 2, 364-382.
(41) Ditchfield, R.; Hehre, W. J.; Pople, J. A. *J. Chem. Phys.*, **1971**, 54, 724-728.
(42) Koelsch, C. F.; Anthes, J. A. *J. Org. Chem.* **1941**, 6, 558-565.

(43) Kruszewski, J.; Krygowski, T. M. *Tetrahedron Lett.* **1972**, 13(36), 3839-3842.
(44) Krygowski, T. M. *J. Chem. Inf. Comp. Sci.* **1993**, 33, 70-78.
(45) Schleyer, P. R.; Maerker, C.; Dransfeld, A.; Jiao, H.; Hommes, N. J. R. v. E. *J. Am. Chem. Soc.* **1996**, 118, 6317-6318.
(46) M.C. Daza, M. Doerr, S. Salzmann, C.M. Marian, W. Thiel, *Phys. Chem. Chem. Phys.* **2009**, 11, 1688-1696.

Authors are required to submit a graphic entry for the Table of Contents (TOC) that, in conjunction with the manuscript title, should give the reader a representative idea of one of the following: A key structure, reaction, equation, concept, or theorem, etc., that is discussed in the manuscript. Consult the journal's Instructions for Authors for TOC graphic specifications.

Insert Table of Contents artwork here